The Astrophysical Journal, 650:1172–1183, 2006 October 20

OBSERVATIONS OF FLUX ROPE FORMATION IN THE OUTER CORONA

Y.-M. Wang and N. R. Sheeley, Jr.
Code 7672, E. O. Hulburt Center for Space Research, Naval Research Laboratory, Washington, DC 20375-5352;
ywang@yucca.nrl.navy.mil, sheeley@spruce.nrl.navy.mil
Received 2006 March 22; accepted 2006 June 12

ABSTRACT

In previous studies employing the Large Angle and Spectrometric Coronagraph (LASCO), we identified a class of white-light ejections that separate into incoming and outgoing components at distances of ~3–5 $R_\odot$ from Sun center. These events, of which up to several per month are observed during high solar activity, are generally preceded by a gradual outward expansion of faint loops over a period of a day or more. The expansion terminates when the streamer material, in the form of an elongated stalk or a sheetlike structure, suddenly tears apart. The collapsing material is sometimes recognizable as a collection of loops, while the ejected component is usually poorly resolved. Here we describe a streamer detachment observed on 2005 December 11, in which the outgoing component can be clearly identified as a cylindrical flux rope with its ends anchored in the Sun. Based on simple three-dimensional white-light reconstructions, we conclude that in/out pairs in general represent the pinching off of streamer loop arcades to form flux ropes, as seen from different viewing angles.

Subject headings: Sun: corona — Sun: coronal mass ejections (CMEs) — Sun: magnetic fields

1. INTRODUCTION

Over the last decade, the Large Angle and Spectrometric Coronagraph (LASCO) on the *Solar and Heliospheric Observatory* (*SOHO*) has detected multitudes of faint white-light features moving inward toward the Sun at heliocentric distances of $r \sim 2$–$6\ R_\odot$ (see Sheeley & Wang 2001, 2002; Sheeley et al. 2001, 2004; Wang et al. 1999a, 1999b). The occurrence rate of these events rose steeply from ~1 day^{-1} during the 1996–1997 sunspot minimum to as many as ~10–100 day^{-1} from late 1998 through 2004, falling again to ~1 day^{-1} by early 2006. The great majority of the inflows have the form of narrow, sinking columns of material, which take on a cusplike appearance below $r \sim 3\ R_\odot$ and leave a dark depletion trail in their wake. These small-scale events are concentrated around warps in the heliospheric current sheet (HCS) and suggest the pinching off and closing down of magnetic flux associated with coronal holes and coronal mass ejections (CMEs). However, the expected outgoing counterparts are rarely observed, perhaps because of their intrinsic faintness and the sensitivity limitations of the LASCO instrument beyond $r \sim 6\ R_\odot$.

In addition to the sinking column inflows, we have identified larger scale (but still relatively faint) events in which both incoming and outgoing components are detected (Wang et al. 1999a; Sheeley & Wang 2002; Simnett 2004). These in/out pairs, of which up to several per month are seen during high solar activity, are preceded by a gradual outward expansion of coronal loops over a period of a day or more (Sheeley & Wang 2006, hereafter Paper II). In some events, a narrow helmet streamer becomes progressively more elongated before splitting apart. In other cases, a hole suddenly develops within a sheet of streamer material, with the outward-moving edge forming an arch-shaped front and the downward-moving component sometimes resolving into a collection of loops. As shown in Paper II, arch-shaped ejections are also observed without collapsing counterparts; here the separation may have occurred below or near the inner edge of the $r \gtrsim 2\ R_\odot$ field of view of the LASCO C2 coronagraph.

The outgoing component of an in/out pair is usually difficult to resolve spatially. A striking exception is provided by a helmet streamer event on 2005 December 11, which is described in §§ 2 and 3. In § 4, we construct a simple three-dimensional model for the white-light structure formed after the streamer loops have reconnected with each other. Generalizing, we deduce that the outgoing component in both streamer detachments and archlike ejections is a cylindrical flux rope with both ends still attached to the Sun (§ 5). Our results are summarized and their implications discussed in § 6.

2. HELMET STREAMER EVENT OF 2005 DECEMBER 11

The LASCO instrument (Brueckner et al. 1995) currently consists of two white-light coronagraphs with overlapping fields of view, C2 ($2\ R_\odot \lesssim r \lesssim 6\ R_\odot$) and C3 ($4\ R_\odot \lesssim r \lesssim 30\ R_\odot$). Each component is equipped with its own 1024×1024 pixel CCD camera, which records images with a 2 pixel resolution of 24″ (C2) and 112″ (C3). During 2005 December 10–11, C2 (C3) images were taken at a rate of five (two) per hour.

The streamer disruption event occurred above the Sun's northwest limb at a position angle P.A. $\simeq 310^\circ$. The sequence of LASCO C2 images in Figures 1 and 2 shows the evolution of the streamer between 0824 UT on 2005 December 10 and 0712 UT on the next day. Here, to remove the contributions of the F corona and instrumental stray light, the left-hand images were processed by subtracting a background representing the minimum intensity recorded within each pixel during the given solar rotation. The corresponding edge-enhanced images on the right were constructed by subtracting a smoothed version of the left-hand image from itself.

The helmet streamer begins its slow outward expansion ~1–2 days before the first observation shown in Figure 1. As they drift outward at speeds of a few tens of kilometers per second, the loops become increasingly elongated and begin to take on a linear, raylike appearance. As the envelope of the streamer continues to open up and fade, its core, in the form of a succession of narrow, tightly packed loops, gradually emerges into the $r \gtrsim 2\ R_\odot$ field of view during the latter part of December 10. The legs of the arcade loops pinch inward as the loop tops rise, so that by 0224 UT on December 11 the helmet streamer has been transformed from a

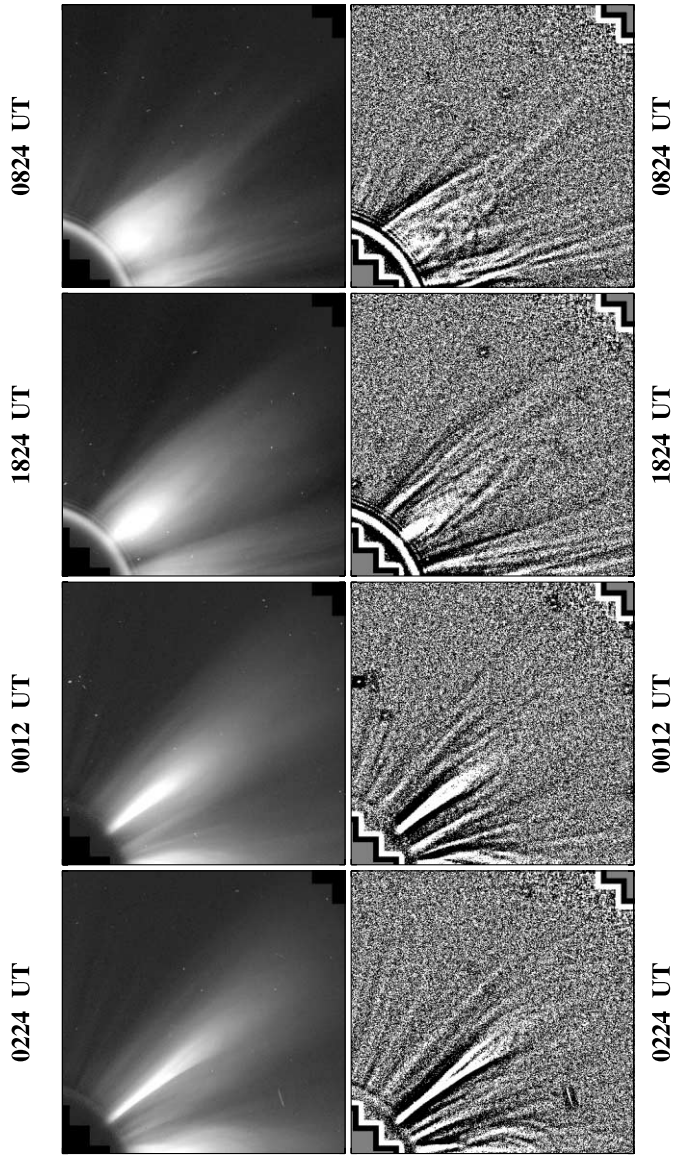

FIG. 1.—Time sequence of LASCO C2 images, showing the gradual expansion and elongation of a helmet streamer above the Sun's northwest limb on 2005 December 10–11. Time runs from top to bottom; the occulting disk extends out to $r \sim 2\ R_\odot$. *Left column*, Images processed by subtracting a background consisting of the minimum intensity recorded at each pixel location during the given solar rotation; *right column*, unsharp mask images, obtained by subtracting from each left-hand image a spatially smoothed version of itself.

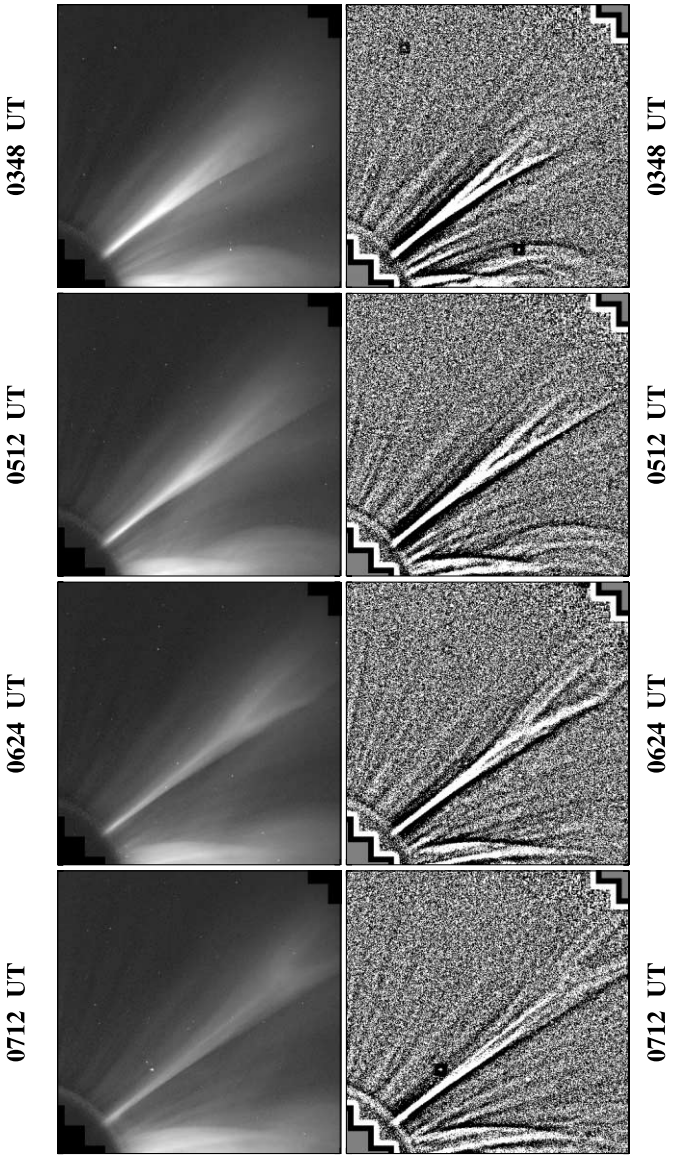

FIG. 2.—Continuation of the time sequence in Fig. 1, showing the formation of a V-shaped feature early on December 11. *Left column*, C2 images with background minimum subtracted; *right column*, corresponding unsharp mask images.

broad, domelike structure into a slender, diverging stalk. By 0348 UT (Fig. 2), the fading stalk begins to develop a fork, which widens progressively while moving outward with increasing speed. The fork remains connected to the Sun by the faint stalk, although the width of the stalk decreases to only $\sim 2^\circ$.

In Figure 3, we see the V-shaped structure rising through the LASCO C3 field of view beyond $r \sim 4\ R_\odot$. The "V" continues to flatten out, its bottom catching up with its sides. By 0942 UT, the structure has the appearance of a cone with a more or less circular cross section. The vertex of the cone remains attached to the Sun. (Fig. 5 in Wang et al. [1999a] shows a somewhat similar, claw-shaped feature moving through the C3 field following a streamer detachment event on 1996 September 7.)

The evolution of the streamer can also be studied by subtracting from each image the one preceding it, so as to bring out the changes that occur from one moment to the next. By extracting from each successive running-difference image a radial strip aligned along the streamer axis and arranging the strips in a time-ordered sequence, we may construct a height-time map. Figure 4 shows the result obtained using LASCO C2 images recorded between ~2300 UT on December 10 and ~0700 UT on December 11. The narrow loops of the streamer core are seen rising through the field of view, forming teardrop structures as their legs pinch inward. After ~0300 UT, the legs appear to pinch off, and the trailing ends of the loops take on a V shape. (Since the latter feature remains connected to the Sun by the thin stalk seen in Figure 2, the pinching off evidently involves three-dimensional reconnection between neighboring streamer loops, not the complete disconnection of magnetic flux that would occur in an idealized two-dimensional system.) At the same time, one or more faint downward tracks (whose slopes correspond to speeds of order 100 km s^{-1}) can be seen diverging from the upward track of the V-shaped structure. Both the incoming and outgoing material leave density depletions in their wake. A backward extrapolation of the tracks to their point of intersection suggests that the pinching off occurs near $r \sim 3\ R_\odot$ between ~0300 and ~0400 UT.

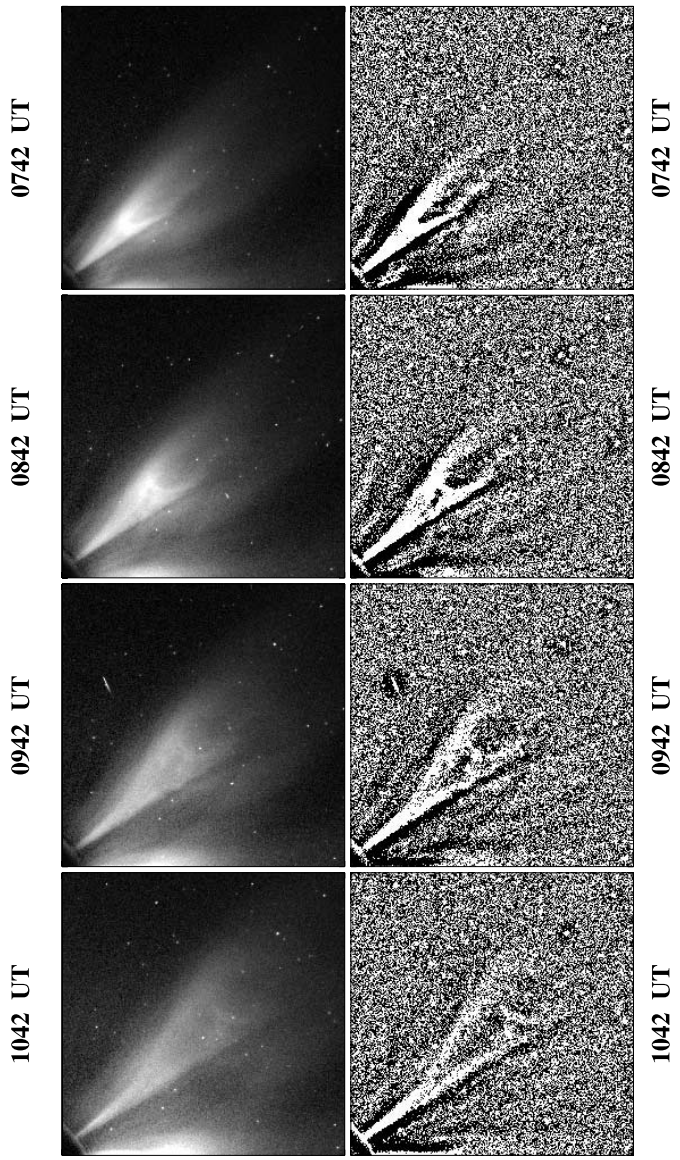

FIG. 3.—Continuation of the time sequence in Fig. 2, showing the concave-outward structure entering the LASCO C3 field of view between $r \sim 4\ R_\odot$ and $r \sim 20\ R_\odot$. *Left column*, C3 images with background minimum subtracted; *right column*, corresponding unsharp mask images.

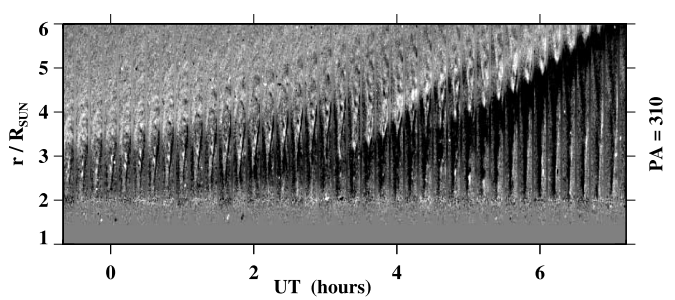

FIG. 4.—Height-time map, showing the pinching off of the helmet streamer loops early on 2005 December 11. The map was constructed by extracting a radial strip centered along the streamer axis (P.A. = 310°) from each of a succession of C2 running-difference images and arranging the vertically oriented strips in a time-ordered sequence. White (black) means that the local intensity has increased (decreased) since the observation taken 12 minutes earlier.

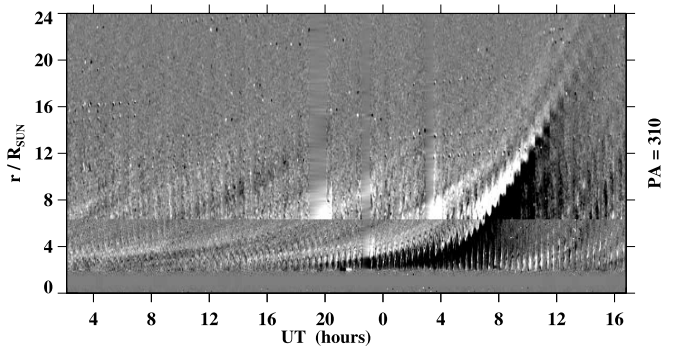

FIG. 5.—Composite height-time map, showing the evolution of the helmet streamer out to $r = 24\ R_\odot$ during 2005 December 10–11. The map was constructed using both C2 and C3 running-difference images.

Figure 5 shows a composite height-time map constructed using both C2 and C3 observations from ~0200 UT on December 10 to ~1700 UT on December 11. The slow expansion of the streamer envelope during December 9–10 produces a multitude of faint, gently curving tracks traversing the C2 and C3 fields of view. The narrow loops in the streamer core initially follow a similar, slowly accelerating trajectory; however, the slope suddenly steepens when the inner loops pinch off early on December 11. The V-shaped trailing end (which, as noted above, remains connected to the Sun) accelerates outward, eventually merging with the slower moving material ahead of it; the asymptotic slope of the merged tracks corresponds to a final speed of ~400 km s^{-1}. The days-long streamer expansion shuts off after the passage of this clean-out front. The subsequent tracks seen on December 11 are produced by a succession of narrow streamer blobs (Sheeley et al. 1997; Wang et al. 1998), rather than by outward-drifting loops.

The latitude-longitude maps in Figure 6 provide a synoptic view of the white-light streamer belt and its evolution between Carrington rotations (CRs) 2037 and 2038. To construct each map, slices of east- or west-limb data centered at $r \simeq 3\ R_\odot$ were extracted from individual background-subtracted C2 images and assembled into a time-reversed sequence spanning the given rotation. The disruption of the helmet streamer on December 11 takes the form of a sudden narrowing and dimming of the intensity pattern at longitude $\phi \sim 240^\circ$ and latitude $L \sim 40^\circ$ in the west-limb map for CR 2037 (Fig. 6, *middle*). Half a rotation earlier, the streamer appears as part of a bright, stable structure in the east-limb map for CR 2037 (Fig. 6, *top*). Half a rotation after the event, we again see a bright structure at the east limb, but shifted equatorward by ~10° (Fig. 6, *bottom*). Apparently, the helmet streamer re-formed at a lower latitude while on the back side of the Sun.

3. RELATIONSHIP TO THE PHOTOSPHERIC AND CORONAL FIELDS

Figure 7 shows the photospheric field and the Fe XV λ284 corona in the region below the helmet streamer, as they appeared on 2005 November 5, December 2, and December 29. The magnetograms are from the *SOHO* Michelson Doppler Imager (MDI; Scherrer et al. 1995), while the Fe XV images are from the *SOHO* Extreme-Ultraviolet Imaging Telescope (EIT; Delaboudinière et al. 1995). (No EIT observations were taken during December 3–17.) On November 5, the area is dominated by a large, decaying bipolar magnetic region (BMR). One rotation later, several smaller active regions have emerged within or near the bipolar remnant. When the complex reappears on December 29, the new bipoles

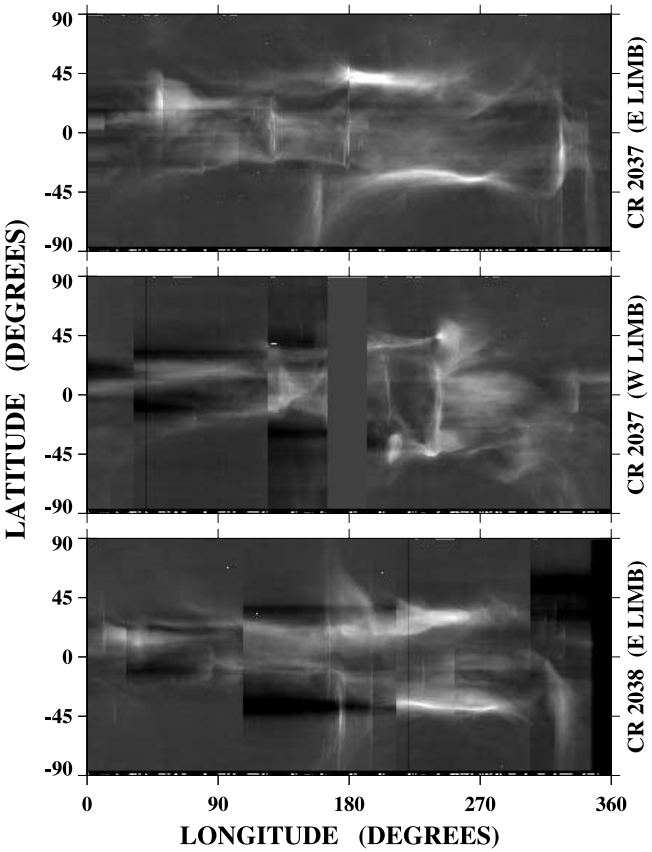

FIG. 6.—Carrington format maps, showing the white-light streamer structures at the east limb during CR 2037 (*top*), the west limb during CR 2037 (*middle*), and the east limb during CR 2038 (*bottom*). The maps were constructed from individual LASCO C2 images by extracting from each background-subtracted image a slice of east- or west-limb data centered at $r \simeq 3\ R_\odot$ and arranging the strips in a time-reversed sequence. The disruption of the helmet streamer on December 11 is seen as a sudden constriction and fading of the brightness pattern at $\phi \sim 240^\circ$, $L \sim 40^\circ$ in the west-limb map.

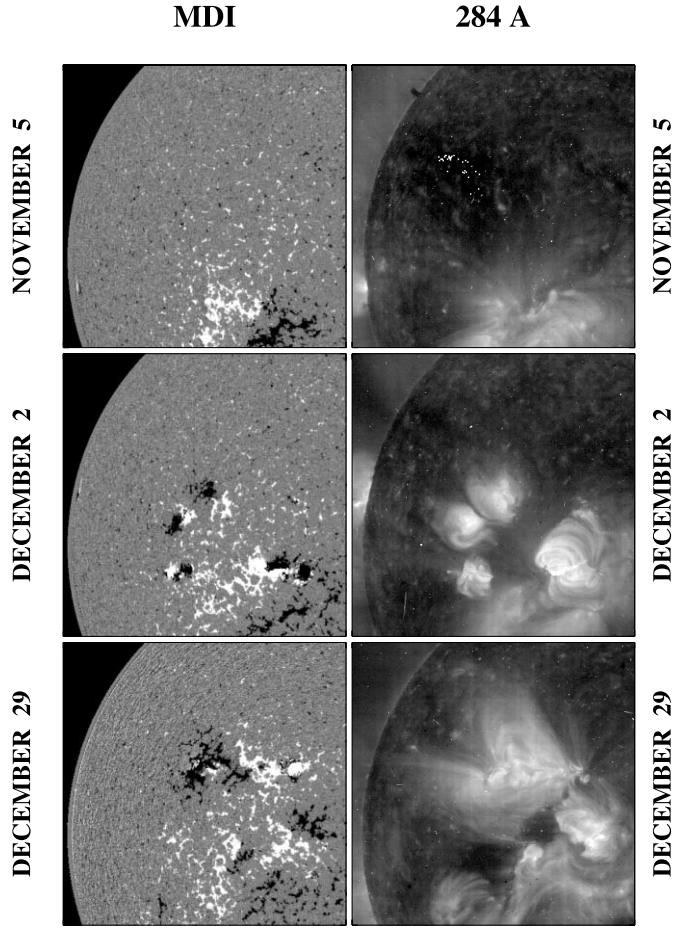

FIG. 7.—Observed evolution of the photospheric field and corona below the helmet streamer during 2005 November and December. *Left column*, MDI Ni I λ6768 magnetograms recorded on November 5, December 2, and December 29; *right column*, corresponding EIT Fe XV λ284 images.

have decayed, but a large east-west–oriented BMR is now present near latitude 10° north. While most of the new northern hemisphere activity occurred on the back side of the Sun after December 11, MDI and National Solar Observatory (NSO) magnetograms show some flux beginning to emerge at this location as early as December 9–10. Also during the interval between December 2 and 29, a dark Fe XV coronal hole developed within the positive-polarity area around the equator. A weaker hole, obscured by the overlying Fe XV emission, but visible in NSO He I λ10830 spectroheliograms, was probably present in this region on December 2.

The coronal field configuration in the vicinity of the helmet streamer can be deduced by applying a potential field source surface (PFSS) extrapolation to the observed photospheric field. In the PFSS model (Schatten et al. 1969), the corona is assumed to remain current-free out to a spherical "source surface" at $r = R_{\rm ss} \simeq 2.5\ R_\odot$, where the nonradial field components are set to zero, simulating the magnetohydrodynamic effect of the solar wind. At the inner boundary $r = 1\ R_\odot$, the radial component B_r of the potential field is matched to the photospheric field, which is taken to be radially oriented at the depth where it is measured (Wang & Sheeley 1992). All field lines that extend from the photosphere to the source surface are defined as open; their footpoint areas generally coincide with He I λ10830 coronal holes (see Wang et al. 1996, Fig. 2). We emphasize that this model is not intended to describe the actual magnetic topology of the streamer at the time of the event, but only the global, time-averaged distribution of the coronal field during the given solar rotation.

Figure 8 displays the field line configuration above the Sun's northwest limb on 2005 December 9, as derived using the Mount Wilson Observatory (MWO) photospheric field map for CR 2037. A large, well-ordered loop arcade is centered at the latitude ($L \sim 40^\circ$) of the observed helmet streamer. The arcade is bounded on each side by open field lines (color-coded green) rooted, respectively, in the negative-polarity polar coronal hole and in a positive-polarity equatorial region. A closer examination reveals that the arcade has an octupolar structure, with three underlying neutral lines, as in the magnetic breakout configuration of Antiochos et al. (1999).

Figure 9 (*left column*) compares the PFSS field line configurations for November 12, December 9, and January 5, computed using the MWO photospheric maps for CR 2036, 2037, and 2038 (whose respective starting dates are 2005 October 28, November 25, and December 22). The field lines have been traced outward from the same footpoint locations in all three photospheric maps. In the right-hand column, we have also rotated each "hairy ball" image so that the region of interest appears near central meridian, rather than at the northwest limb. Through the entire period, a helmet streamer arcade (defined by the blue field lines) links the negative-polarity polar cap with the strong positive-polarity flux near the equator. In the interval between November 12 and December 9, a small region of strong negative-polarity flux emerges beneath the equatorward leg of the

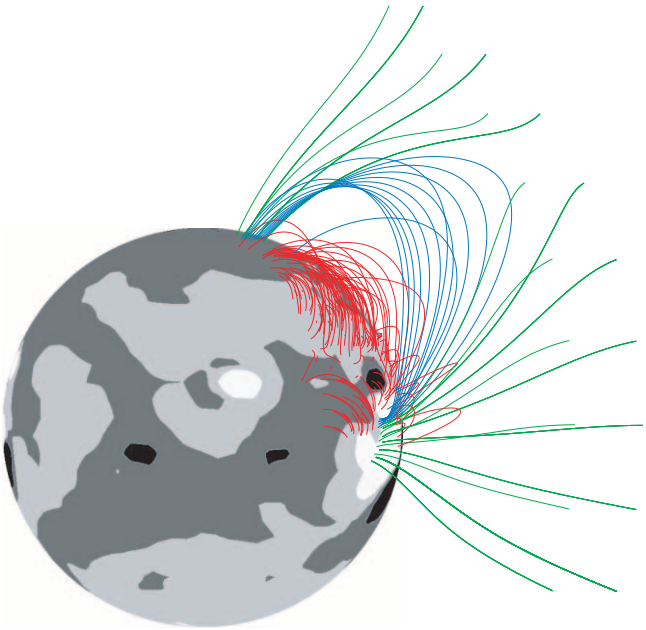

FIG. 8.—Coronal field-line configuration near the northwest limb on 2005 December 9, as derived by applying a PFSS extrapolation to the MWO photospheric field map for CR 2037. Open field lines are coded green; closed loops are blue if they extend beyond $r = 1.5\ R_\odot$ and red otherwise. Black, dark gray, light gray, and white denote areas of the photosphere where $B_r < -10$ G, -10 G $< B_r < 0$ G, 0 G $< B_r < +10$ G, and $B_r > +10$ G, respectively. Here and in the following two figures, the magnetograph data have been corrected for the saturation of the Fe I λ5250 line profile, as described in Wang & Sheeley (1995).

streamer. The overlying arcade loops are "repelled" toward the source surface, and new open field lines are created, with footpoints in the negative-polarity polar hole and the positive-polarity equatorial hole (compare the hairy-ball plots for November 12 and December 9). (In an MHD description, the outward expansion would be driven by the increase in magnetic and thermal pressure accompanying the injection of flux at the inner boundary.) Between December 9 and January 5, a large BMR emerges just north of the equator, greatly strengthening the negative-polarity region under the streamer. As a result, more polar cap field lines open up at this longitude, and the polar hole boundary advances toward the negative-polarity sector of the BMR (while receding from the positive-polarity sector farther to the west). At the same time, some of the open field lines on the equatorward side of the streamer close down and are transferred northwestward toward the positive-polarity sector of the BMR. Although the process itself is not described by the PFSS model, this transfer presumably occurs through reconnection (footpoint exchange) between neighboring open and closed field lines (see Wang & Sheeley 2004; Crooker et al. 2002). The net effect is to shift the helmet streamer to lower latitudes, consistent with the LASCO observations.

The change in the latitude of the helmet streamer can also be understood in terms of the evolution of the source surface neutral line, defined by $B_r(R_{ss}, L, \phi) = 0$. As demonstrated in Wang et al. (1997), the white-light streamer structure beyond $r \sim 2.5\ R_\odot$ is produced by Thomson scattering of photospheric radiation from a thin plasma layer centered on the HCS, whose angular position coincides with that of the source surface neutral line. In the left column of Figure 10 we display the photospheric and source surface fields for CR 2037 as a function of latitude and longitude, along with the simulated and observed west-limb streamer intensities at $r \simeq 3\ R_\odot$; the right column shows the corresponding maps for CR 2038, except that the streamer patterns are now as they appear at the east, rather than the west, limb. In general, if CMEs and other transient effects are ignored, the brightest white-light structures occur where the source surface neutral line is horizontal ($dL_{ssnl}/d\phi = 0$); at these stationary points, the HCS/plasma sheet is viewed edge-on and the electron column density along the line of sight is greatest. The helmet streamer of December 9–11 is located where the neutral line has its maximum northward extension; this warp is in turn associated with the activity complex at $\phi \sim 240^\circ$. The large BMR that emerges in the northern hemisphere between CR 2037 and 2038 has east-west polarity orientation opposite to that of the active region remnant in the south. As a result, the net equatorial dipole moment decreases, and the latitudinal excursion of the source surface neutral line is somewhat reduced. As indicated by Figure 10, the predicted and observed changes in the streamer locations are in reasonable agreement.

In summary, we suggest that flux emergence under the helmet streamer led to its outward expansion and disruption during December 9–11, as well as to its subsequent re-formation at lower latitudes. Footpoint shearing by photospheric differential rotation may also have contributed to the destabilization of the streamer arcade (as simulated numerically by Linker & Mikić 1995), while simultaneously strengthening the axial field component required for flux rope formation.

4. THREE-DIMENSIONAL RECONSTRUCTION OF THE STREAMER EJECTION

We now demonstrate that concave-outward structures such as those seen in Figures 2 and 3 can be produced by scattering from the surface of a curved, hollow tube whose ends are anchored on the Sun. The axis of this idealized tube has its midpoint and apex located at heliocentric distance $r = r_m$ and longitude $\phi = \phi_m$, while its endpoints are positioned at $r = 1\ R_\odot$ and $\phi = \phi_m \pm \Delta\phi$. For simplicity, we also suppose that the axis is confined to a single latitude, $L = L_{axis}$. The cross sections of the tube are closed curves that are centered on the axis, lie in meridional planes, and expand with axial distance. The coronal plasma is assumed to be concentrated uniformly along these closed curves, and the formulae of Billings (1966) are again used to calculate the distribution of white-light radiation Thomson-scattered into the line of sight (see also Wang et al. 1997).

Consider first the case of a circular cross section, defined by $x = a\cos\xi$ and $y = a\sin\xi$, where $0 \le \xi \le 2\pi$ and a increases with axial distance from the Sun. For illustrative purposes, we set $L_{axis} = 40^\circ$ and position the axis so that its midpoint and apex lie directly above the Sun's west limb at $r_m = 5\ R_\odot$; we also set $\Delta\phi = 20^\circ$, so that the endpoints are separated by 40° in longitude. Figure 11 shows how the structure would appear as seen from Earth (*top*) and from above the Sun's north pole (*bottom*). In the Earth-based view (where the axis is normal to the sky plane), we see a hollow, cone-shaped structure. The sunward surface is relatively bright because of the radial convergence of the circular cross sections (which are more tightly bunched on the inward side). Because the endpoints are symmetrically placed on each side of the solar limb, the two "legs" of the structure (behind and in front of the sky plane) merge into a single entity in the line of sight. The polar view shows an archlike structure with two tapered legs; the inner and outer edges of the arch are relatively bright because the path length through the curved surface is greatest there.

Now let the cross section of the tube have a teardrop shape $x = a\cos\xi$ and $y = ka^2(1 + \cos\xi)^2\sin\xi$, where $0 \le \xi \le 2\pi$, a

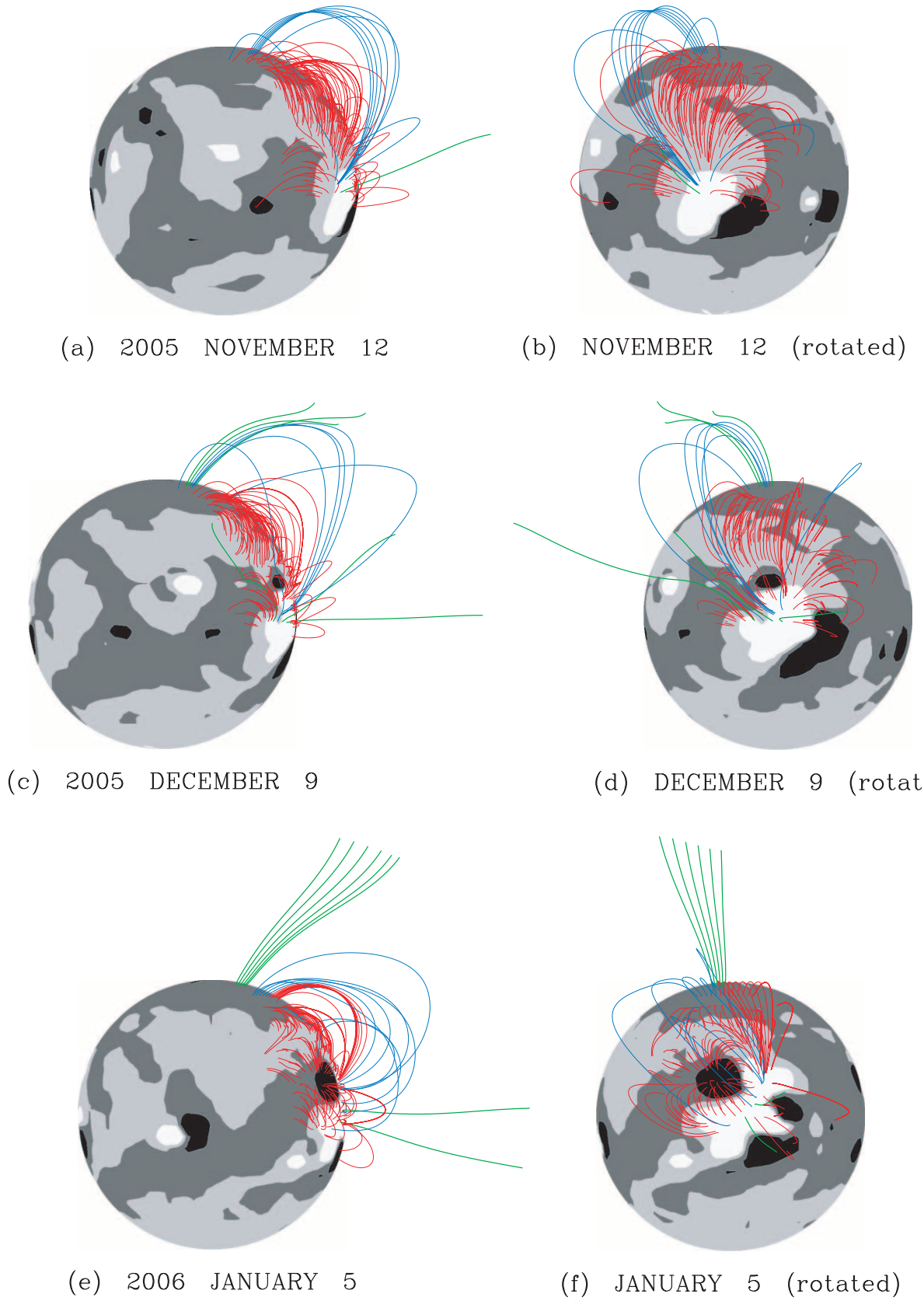

FIG. 9.—Evolving magnetic topology of the helmet streamer, as inferred from a PFSS extrapolation of the MWO photospheric maps for CR 2036 through 2038. *Left column*, Coronal field-line configuration near the northwest limb on November 12, December 9, and January 5; *right column*, same as left column, but rotated so that the region of interest lies near central meridian. Field lines have been traced outward from the same footpoint locations (regularly spaced in sine latitude and Carrington longitude) in all three photospheric maps.

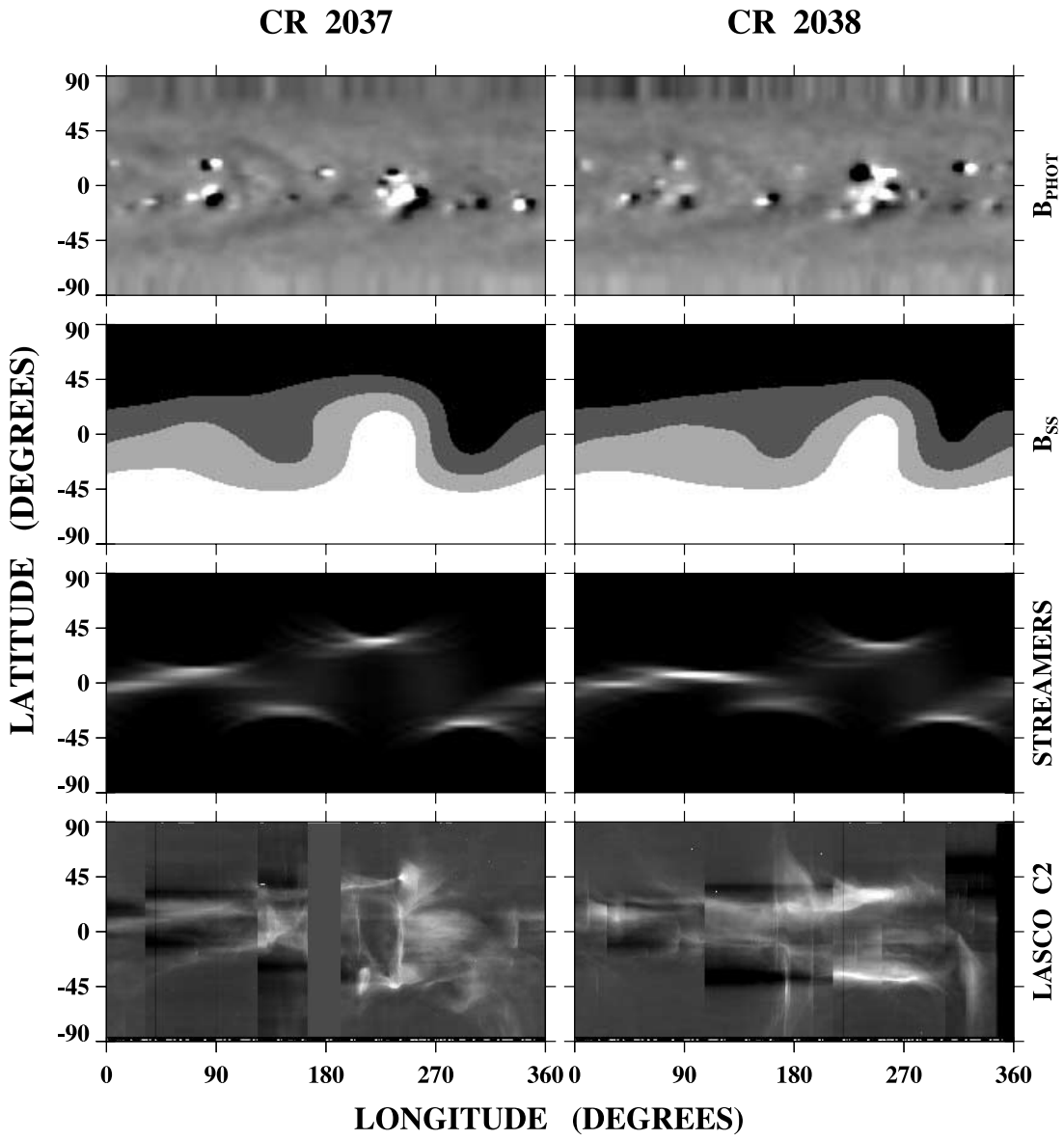

FIG. 10.—*Left*: Latitude-longitude maps for CR 2037, showing the MWO photospheric field, source surface field, simulated west-limb streamer patterns, and LASCO C2 brightness distribution above the west limb at $r \simeq 3\ R_\odot$. *Right*: Corresponding maps for CR 2038, with the simulated and observed streamers now at the east, rather than the west, limb. Gray scale for the photospheric field ranges from $B_r < -30$ G (*black*) to $B_r > +30$ G (*white*). In the source surface maps, black, dark gray, light gray, and white denote $B_r < -0.2$ G, -0.2 G $< B_r < 0$ G, 0 G $< B_r < +0.2$ G, and $B_r > +0.2$ G, respectively. The simulated streamer patterns were produced by Thomson scattering of photospheric radiation from a 4° wide plasma sheet extending radially outward from the source surface neutral line.

increases with axial distance, k is a constant, and the cusp point $\xi = \pi$ is located on the sunward side. Setting $r_m = 4.5\ R_\odot$ and $\Delta\phi = 20^\circ$ and again positioning the midpoint of the axis above the west limb, we obtain the results displayed in Figure 12. Looking from Earth, we see a bright, Y-shaped structure representing the pinched-in underside of the three-dimensional teardrop surface; the pointed cusps line up to form the stem of the Y. The view from the pole shows an archlike structure resembling that in of Figure 11 (*bottom*), except that the inner edge of the arch is now fainter, because the path length through the cusp point is smaller than through the circular rim.

In Figure 13, we have repeated the simulation of Figure 12, with the midpoint of the axis located 15° in front of, rather than directly above, the west limb. The Earth-based observer now sees both legs of the tube, which are no longer exactly aligned along the line of sight. (The legs appear to be separated in latitude because the sky-plane projected position of a given feature depends on its longitudinal distance from the limb.)

Comparing Figure 12 with Figure 2, we conclude that the Y-shaped structure that forms early on December 11 can be modeled as a hollow tube whose axis is perpendicular to the sky plane and that is pinched inward on its sunward side. The tube has at least one end anchored in the Sun, and its cross-sectional area increases with heliocentric distance. The hollow appearance of the observed structure is presumably a result of the inner loops of the flux rope pinching off and fading before the outer ones.

Similarly, a comparison of Figures 3 and 11 suggests that the cone-shaped structure observed in the LASCO C3 field of view represents a Sun-anchored tube with a circular cross section that expands with height. Evidently, the originally V-shaped underside of the tube has now flattened out.

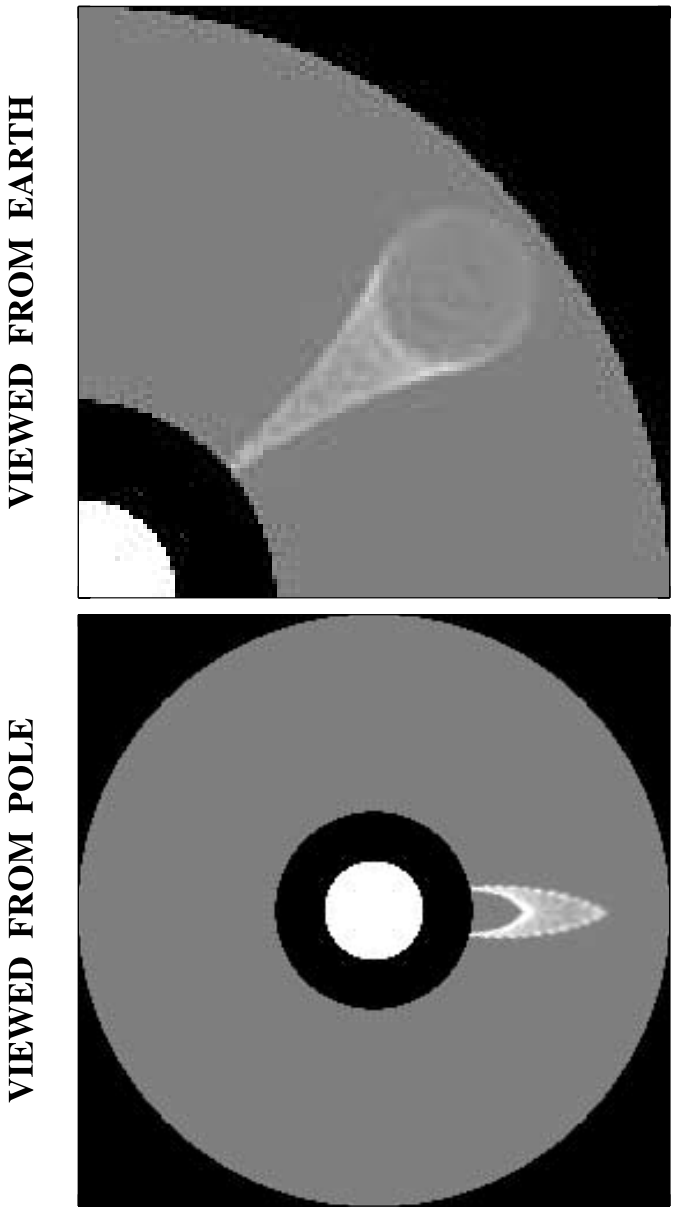

FIG. 11.—Two views of a hollow tubular structure with circular cross section and both ends anchored at latitude +40° on the Sun. The Thomson-scattering electrons are concentrated on the surface of the tube, whose curved axis is symmetric about the west limb and whose cross section expands with axial distance from the Sun. *Top*, Earth-based view, in which the axis of the tube is perpendicular to the sky plane; *bottom*, view from the Sun's north pole, in which the axis is parallel to the sky plane.

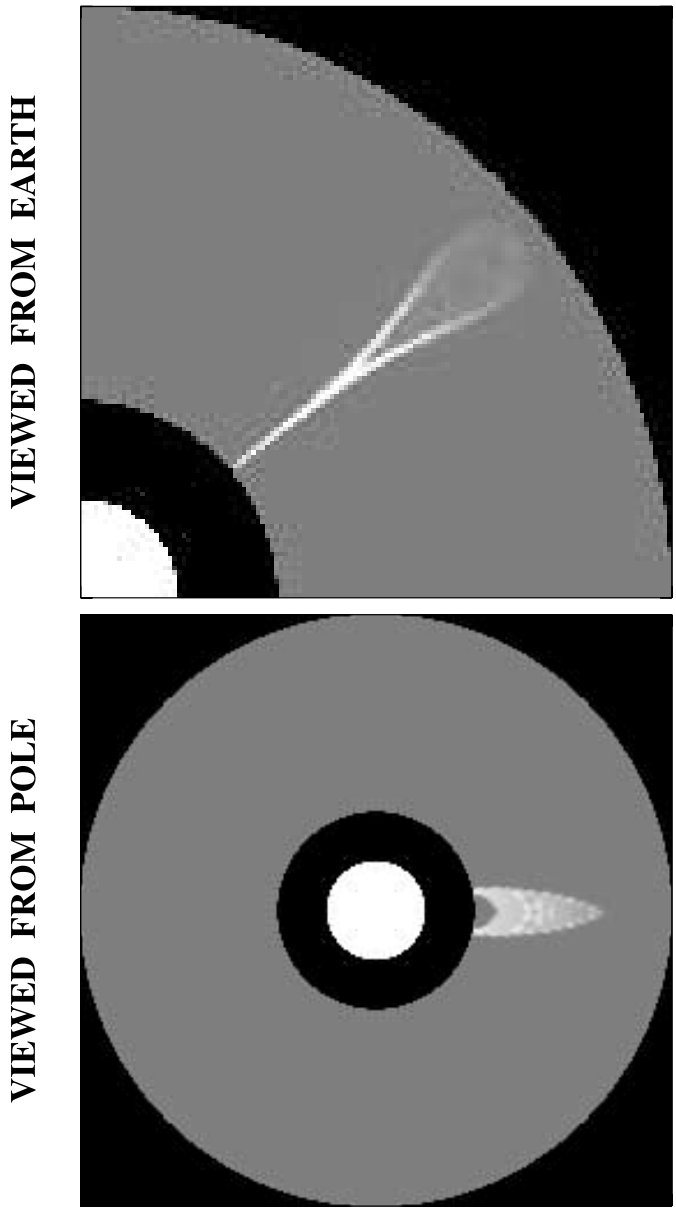

FIG. 12.—Same as Fig. 11, except that the curved tube now has a teardrop cross section that expands with axial distance.

We note that the core regions of CMEs often take on a conelike appearance after fully emerging into the coronagraph field of view. The frequent presence of filamentary structure concentric about the axis of the cone suggests that we are indeed observing a flux rope with cylindrical/toroidal symmetry (cf. Chen et al. 2000; Vourlidas et al. 2000; Wood et al. 1999; Wu et al. 1997). A typical example is shown by the gradually accelerating CME in Figure 14 (*top*); also displayed is a slow, V-shaped ejection (Fig. 14, *bottom*), whose topology again suggests a flux rope. As argued by Gosling et al. (1995), such structures can be produced by three-dimensional magnetic reconnection in erupting loop arcades.

Wu et al. (1997) have presented MHD simulations of a gradually accelerating flux rope CME that traversed the LASCO field of view on 1996 July 28–29. In their axisymmetric model, the concave-outward structure is already present in the preevent corona, where the base of the helmet streamer has the inverse-polarity topology described by Low (1996); the flux rope is then destabilized by increasing its axial field strength while decreasing its internal density. In the 2005 December 11 streamer event, however, the concave-outward feature forms by reconnection near $r \sim 3\ R_{\odot}$ after the destabilization of the streamer arcade.

5. PINCH-OFF AND FLUX ROPE FORMATION FROM DIFFERENT VIEWING ANGLES

Figure 15 shows three examples of in/out pairs observed with the LASCO C2 coronagraph; in each case, we have differenced a pair of images taken roughly half an hour apart. In the event of 1998 May 17 (Fig. 15, *top*), as in that of 2005 December 11, an elongated streamer splits apart; the ejected structure again appears to remain connected to the Sun, while the collapsing material takes the form of an outward-pointing spike (see also Wang et al. 1999a). In the 2001 August 13 event (Fig. 15, *middle*), the

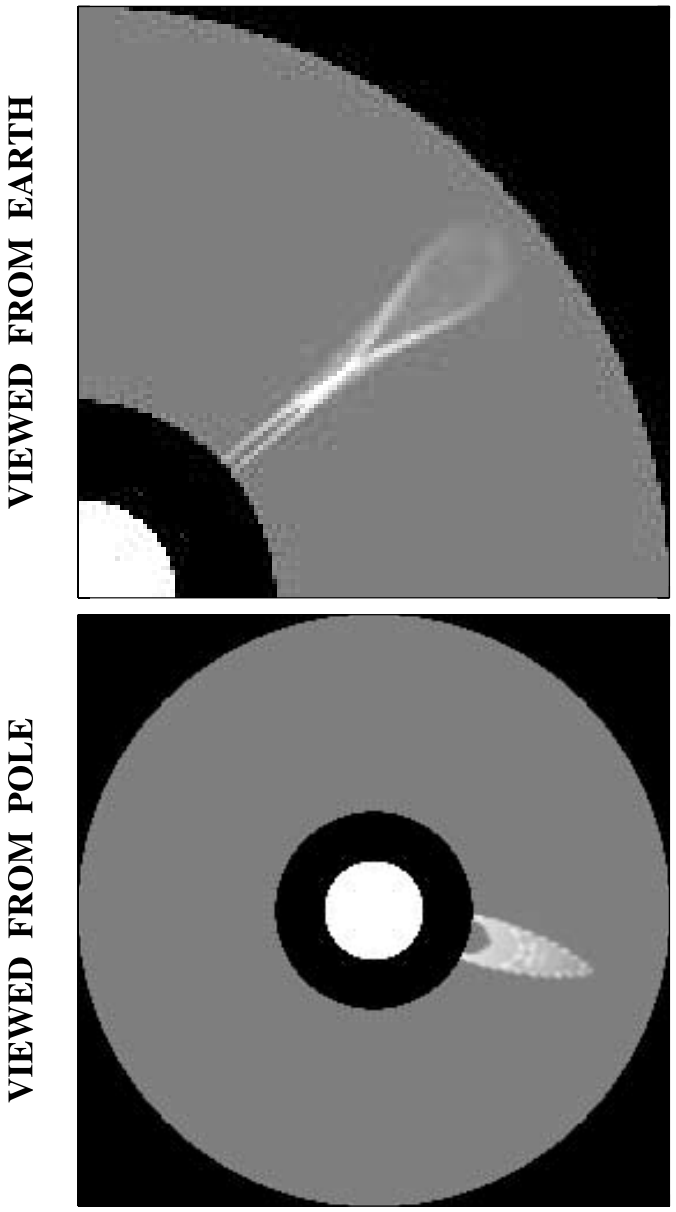

FIG. 13.—Same as Fig. 12, except that the axis of the curved tube is now centered 15° in front of the sky plane (as seen from Earth).

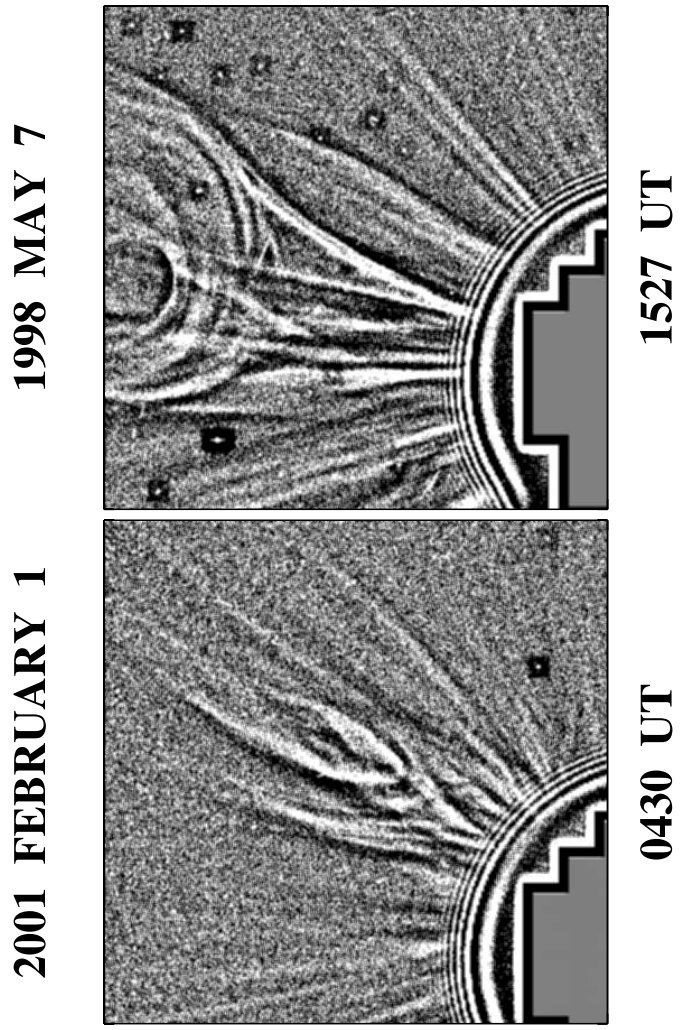

FIG. 14.—Unsharp mask images of flux ropes observed with LASCO C2. *Top:* Example from 1998 May 7, illustrating how the core regions of slow, gradually accelerating CMEs (streamer blowouts), often take on a conelike appearance after emerging fully into the C2 field of view. *Bottom:* Slowly rising streamer structure with teardrop cross section.

in/out pair is observed as an elongated, rapidly diverging oval structure, while in the 2002 August 27 event (Fig. 15, *bottom*) we see a broader expanding oval. In both of these cases, the ejected component forms an arch with both legs rooted in the Sun, resembling the simulated white-light structures in the bottom panels of Figures 11–13, where the axis of the flux rope is parallel, rather than perpendicular, to the sky plane. We therefore interpret Figure 15 as showing the formation of flux ropes from three different viewing angles. In the May 17 event, we are looking directly along the axis of the flux rope (and of the collapsing loop arcade); in the August 13 event, the axis is more skewed with respect to the line of sight; the August 27 event is viewed in a direction nearly perpendicular to the axis, with the flux rope lying almost in the sky plane.

In those cases in which it can be resolved spatially, the inward-moving component of an in/out pair generally consists of one or more cusp-shaped features. The outward-pointing cusps become more rounded and looplike as they approach the inner edge of the C2 field of view, suggesting a relaxation of magnetic tension following reconnection at greater heights. An example from 2001 October 12 is shown in Figure 16. Here the characteristic oval pattern is seen diverging from a point near $r \sim 4\,R_\odot$, where the pinch off of the original loop arcade appears to be initiated and subsequently proceeds eastward and westward along its axis.

Whereas the collapsing component of an in/out pair is more easily observed when the pinch off occurs well above the inner edge of the field of view (at $r \sim 2\,R_\odot$), the opposite holds for the outgoing component, which tends to be better resolved if it is formed at lower heights. In the 2003 August 13 event displayed in Figure 17 (*top*), the separation occurred near $r \sim 3\,R_\odot$, and the inward component has already disappeared behind the LASCO C2 occulter. The twisted or knotted appearance of the archlike front suggests a flux rope. In the morphologically similar event shown in Figure 17 (*bottom*), no collapsing counterpart was observed, presumably because it remained hidden behind the occulting disk. Again, however, the ejected structure has the undulating appearance of a helical flux rope.

As we have already seen in relation to the 2005 December 11 event (and as will be established more generally in Paper II), in/out pairs are preceded by a slow, gradual expansion of faint loops through the outer corona over a period of a day or more. The expansion terminates with the sudden appearance of a gap or hole

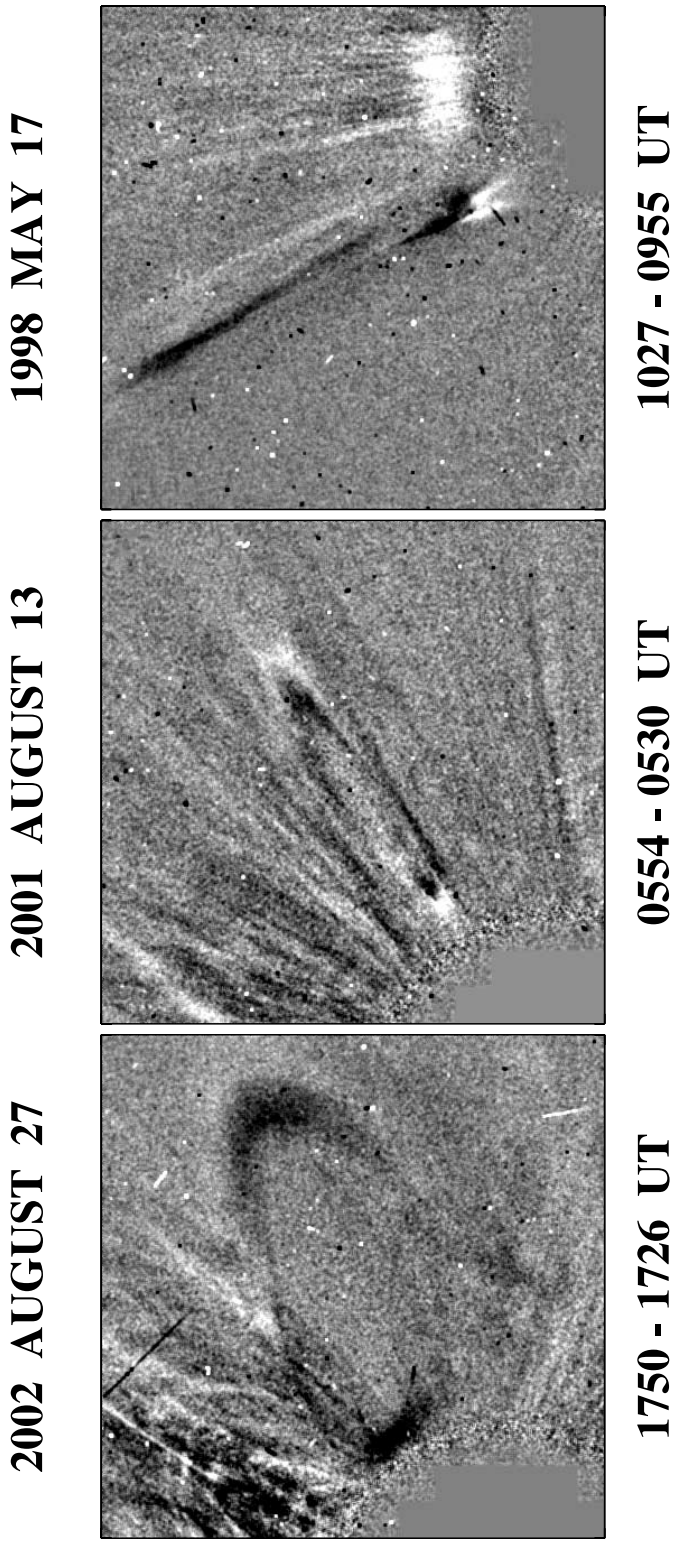

FIG. 15.— In/out pairs observed in the region $r \sim 2$–$6\ R_\odot$. *Top*, 1998 May 17; *middle*, 2001 August 13; *bottom*, 2002 August 27. Each frame shows the difference between two successive LASCO C2 images; white (black) means that the local intensity has increased (decreased) during the intervening time. The morphological similarities between the three events suggest that we are viewing streamer detachments (flux rope formation) from different angles.

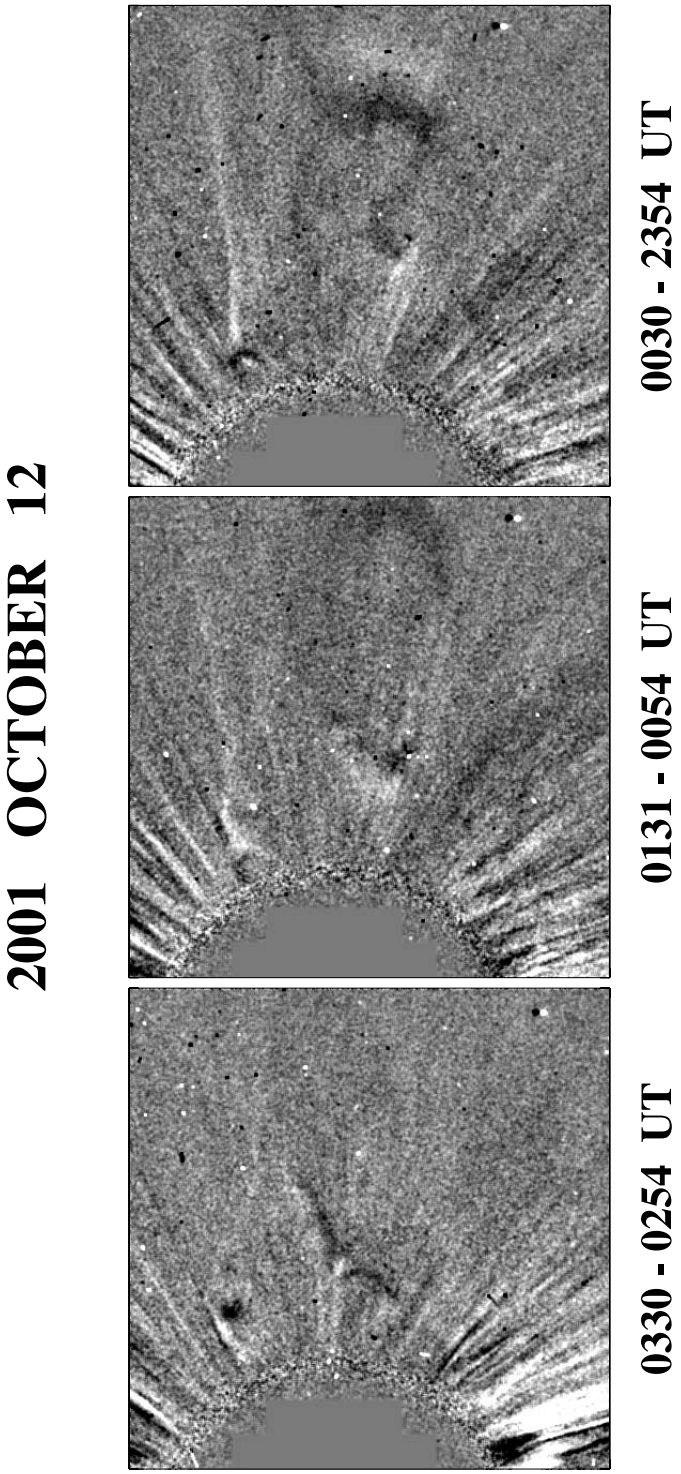

FIG. 16.— In/out pair observed on 2001 October 12, in which the collapsing component resolves into a collection of loops. Each panel represents the difference between two LASCO C2 images taken ~36 minutes apart.

bounded by an in/out pair. In some cases, the event appears to be triggered when a nearby CME perturbs the outward-drifting streamer material (cf. McComas et al. 1991). The two components separate with a relative velocity as high as ~300–400 km s^{-1}, comparable to the local Alfvén speed (see Wang et al. 1999a; Simnett 2004). The collapsing component decelerates from its initial speed of order 100 km s^{-1} as it approaches the inner edge of the C2 field of view, while the ejected component accelerates and eventually coalesces with the slower moving streamer material ahead of it, reaching a final speed of order 400 km s^{-1}. A typical height-time map is displayed in Figure 18; here the gradual expansion of streamer loops over a 2 day interval ends abruptly with the formation of an in/out pair on 2002 August 27 (shown also in Fig. 15, *bottom*). The similarity between the height-time maps of the 2005 December 11 and 2002 August 27 events (compare Figs. 5

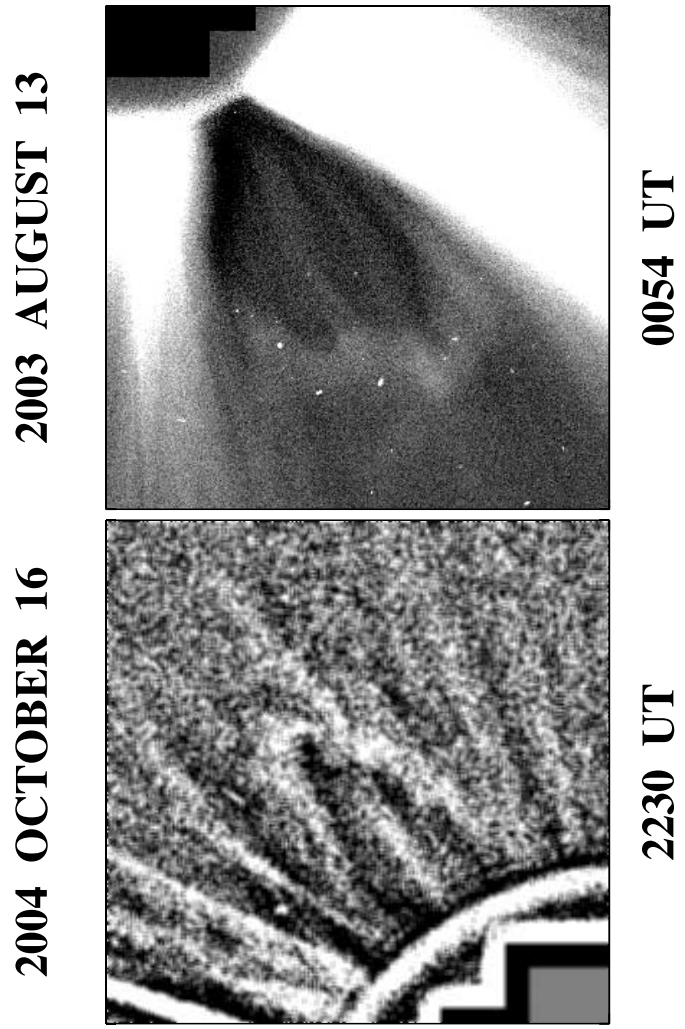

FIG. 17.—Arch-shaped fronts with a characteristic wavy structure suggesting a helical flux rope. *Top*, 2003 August 13 (background minimum subtracted); *bottom*, 2004 October 16 (unsharp mask). No collapsing counterpart was observed in the latter event, presumably because it remained hidden behind the LASCO C2 occulter.

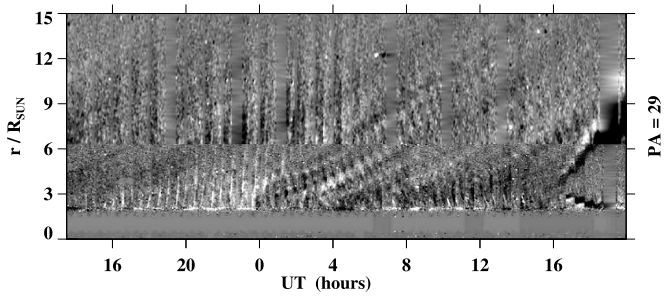

FIG. 18.—Height-time map constructed from C2 and C3 running-difference images, illustrating the gradual expansion of streamer material and its sudden termination with the formation of an in/out pair on 2002 August 27. The clean-out event is also displayed in Fig. 15 (*bottom*).

and 18) again suggests that we are witnessing flux rope formation in streamers from different perspectives.

6. SUMMARY AND DISCUSSION

The main conclusions of this study can be summarized as follows.

1. In/out pairs are produced by the pinching off of streamer loops by magnetic reconnection in the region $r \lesssim 4\ R_\odot$ (see also Wang et al. 1999a; Sheeley & Wang 2002; Simnett 2004; Paper II).

2. The outgoing component is a helical structure (flux rope) with its ends still attached to the Sun, while the incoming component is a collapsing loop arcade.

3. The morphological appearance of the events depends on the viewing angle. If the axis of the helmet streamer arcade coincides with the line of sight, we see a continually elongating streamer stalk that suddenly splits into incoming and outgoing components; in this case, the pinching off occurs at a current sheet that is viewed edge-on. If the axis of the arcade is perpendicular to the line of sight, the current sheet lies in the sky plane and a rapidly expanding hole appears to develop within the streamer material.

4. In the case of the 2005 December 11 event, the gradual evaporation of the helmet streamer and its subsequent re-formation at a lower latitude appear to have been driven by new flux emergence under the streamer.

Just as most ejections observed with the LASCO coronagraph do not show inward-moving counterparts, most inflows do not have detectable outward-moving counterparts. In/out pairs would thus seem to constitute an exceptional class of events. However, structures that resemble flux ropes are often seen entering the C2 field of view from below, including arch-shaped ejections with hollow interiors (Paper II), CME cores with concave-outward topologies (Wood et al. 1999; Chen et al. 2000; Vourlidas et al. 2000), and V-shaped features at the trailing ends of CMEs (Illing & Hundhausen 1983; Webb & Cliver 1995; Simnett et al. 1997; Wu et al. 1997). If these structures are formed by reconnection during the process of eruption, collapsing counterparts should be present below $r \sim 2\ R_\odot$. Indeed, the results of this study and Paper II suggest that in/out pairs and archlike fronts represent "failed" CMEs, in which the outer parts of the streamer arcade are destabilized and open up, but the dense inner core is not ejected; the legs of the overlying loops thus reconnect and pinch off above the core, not below it. Inflows without detectable outgoing counterparts originate at even greater heights ($r \gtrsim 4\ R_\odot$). In this case, open field lines of opposite polarity or the legs of very long streamer loops reconnect with each other, and the ejected U-loops or flux ropes are too faint to be detected with the LASCO C3 coronagraph. Paper II will focus on the relationship between gradual expansions of streamer material, in/out pairs, archlike ejections, and slow CMEs (streamer blowouts).

We thank the LASCO, EIT, and MDI teams for the *SOHO* observations, N. B. Rich and K. Battams for help in constructing the LASCO synoptic maps, and A. F. Thernisien for discussions. The MWO magnetograph data were provided by R. K. Ulrich. This work was supported by NASA and the Office of Naval Research.

REFERENCES

Antiochos, S. K., DeVore, C. R., & Klimchuk, J. A. 1999, ApJ, 510, 485
Billings, D. E. 1966, A Guide to the Solar Corona (New York: Academic)
Brueckner, G. E., et al. 1995, Sol. Phys., 162, 357
Chen, J., et al. 2000, ApJ, 533, 481
Crooker, N. U., Gosling, J. T., & Kahler, S. W. 2002, J. Geophys. Res., 107(A2), SSH 3, DOI: 10.1029/2001JA000236
Delaboudinière, J.-P., et al. 1995, Sol. Phys., 162, 291
Gosling, J. T., Birn, J., & Hesse, M. 1995, Geophys. Res. Lett., 22, 869

Illing, R. M. E., & Hundhausen, A. J. 1983, J. Geophys. Res., 88, 10210
Linker, J. A., & Mikić, Z. 1995, ApJ, 438, L45
Low, B. C. 1996, Sol. Phys., 167, 217
McComas, D. J., Phillips, J. L., Hundhausen, A. J., & Burkepile, J. T. 1991, Geophys. Res. Lett., 18, 73
Schatten, K. H., Wilcox, J. M., & Ness, N. F. 1969, Sol. Phys., 6, 442
Scherrer, P. H., et al. 1995, Sol. Phys., 162, 129
Sheeley, N. R., Jr., Knudson, T. N., & Wang, Y.-M. 2001, ApJ, 546, L131
Sheeley, N. R., Jr., & Wang, Y.-M. 2001, ApJ, 562, L107
———. 2002, ApJ, 579, 874
———. 2006, ApJ, submitted (Paper II)
Sheeley, N. R., Jr., Warren, H. P., & Wang, Y.-M. 2004, ApJ, 616, 1224
Sheeley, N. R., Jr., et al. 1997, ApJ, 484, 472
Simnett, G. M. 2004, A&A, 416, 759
Simnett, G. M., et al. 1997, Sol. Phys., 175, 685
Vourlidas, A., Subramanian, P., Dere, K. P., & Howard, R. A. 2000, ApJ, 534, 456
Wang, Y.-M., Hawley, S. H., & Sheeley, N. R., Jr. 1996, Science, 271, 464
Wang, Y.-M., & Sheeley, N. R., Jr. 1992, ApJ, 392, 310
———. 1995, ApJ, 447, L143
———. 2004, ApJ, 612, 1196
Wang, Y.-M., Sheeley, N. R., Jr., Howard, R. A., Rich, N. B., & Lamy, P. L. 1999a, Geophys. Res. Lett., 26, 1349
Wang, Y.-M., Sheeley, N. R., Jr., Howard, R. A., St. Cyr, O. C., & Simnett, G. M. 1999b, Geophys. Res. Lett., 26, 1203
Wang, Y.-M., et al. 1997, ApJ, 485, 875
———. 1998, ApJ, 498, L165
Webb, D. F., & Cliver, E. W. 1995, J. Geophys. Res., 100, 5853
Wood, B. E., Karovska, M., Chen, J., Brueckner, G. E., Cook, J. W., & Howard, R. A. 1999, ApJ, 512, 484
Wu, S. T., et al. 1997, Sol. Phys., 175, 719